

Research Paper

Novel RNA catalysts for the Michael reaction

Gerhard Sengle^a, Alexander Eisenführ^a, Paramjit S. Arora^b, James S. Nowick^b,
Michael Famulok^{a,*}

^aKekulé-Institut für Organische Chemie und Biochemie, Rheinische Friedrich-Wilhelms-Universität Bonn, Gerhard-Domagk-Straße 1, 53121 Bonn, Germany

^bDepartment of Chemistry, University of California, Irvine, CA 92697-2025, USA

Received 8 January 2001; revisions requested 9 February 2001; revisions received 6 March 2001; accepted 9 March 2001

First published online 27 March 2001

Abstract

Background: In vitro selected ribozymes with nucleotide synthase, peptide and carbon–carbon bond forming activity provide insight into possible scenarios on how chemical transformations may have been catalyzed before protein enzymes had evolved. Metabolic pathways based on ribozymes may have existed at an early stage of evolution.

Results: We have isolated a novel ribozyme that mediates Michael-adduct formation at a Michael-acceptor substrate, similar to the rate-limiting step of the mechanistic sequence of thymidylate synthase. The kinetic characterization of this catalyst revealed a rate enhancement by a factor of $\sim 10^5$. The ribozyme shows substrate specificity and can act as an intermolecular catalyst which transfers the Michael-donor substrate onto an external 20-

mer RNA oligonucleotide containing the Michael-acceptor system.

Conclusions: The ribozyme described here is the first example of a catalytic RNA with Michael-adduct forming activity which represents a key mechanistic step in metabolic pathways and other biochemical reactions. Therefore, previously unforeseen RNA-evolution pathways can be considered, for example the formation of dTMP from dUMP. The substrate specificity of this ribozyme may also render it useful in organic syntheses. © 2001 Elsevier Science Ltd. All rights reserved.

Keywords: Michael-addition; In vitro selection; RNA catalysis; Ribozyme; RNA world

1. Introduction

Research on nucleic acid-based catalysis not only has implications for important biotechnological [1,2] or biomedical applications [3], but also helps to investigate the plausibility of hypotheses on the genesis of early life on earth [4–6]. In vitro selection has proven to be a powerful technology for expanding the scope of catalysis by nucleic acids [7]. We and others took advantage of this approach to isolate catalytically active RNAs (ribozymes) and DNAs (deoxyribozymes) and self-modifying RNAs that accelerate chemical reactions other than phosphodiester bond cleavage or ligation (reviews: [5,7–10]).

Although the Michael-addition reaction is central in both organic chemistry [11] and various cellular processes [12–14] and has been intensively studied, no nucleic acid catalysts for this reaction have been identified. One impor-

tant example represents the initial and rate-limiting step in the mechanistic sequence of the thymidylate synthase, which catalyzes a key step in the biosynthetic pathway of dTMP, i.e. the reductive methylation of dUMP using tetrahydrofolate as the methyl donor. In this system dUMP gets activated via 1,4-Michael-addition reaction in which the Michael-donor, the thiol group of an internal cysteine residue (C198), attacks the Michael-acceptor system of dUMP [15–17].

In the context of the ‘RNA world’ hypothesis, this pathway represents an important link how thymidine synthesis may have occurred from uracil precursors [18,19] in an RNA world in which RNA molecules evolved methods to produce DNA-precursors. An evolutionary experiment for generating RNA molecules catalysing a Michael-addition reaction would contribute new aspects for supporting the ‘RNA world’ hypothesis and, furthermore, would expand the possibilities for catalysis with potential relevance for organic synthesis.

To test whether RNA catalysts could be developed for this important reaction and to provide an RNA model for thymidylate synthase, we designed an in vitro selection

* Correspondence: Michael Famulok;
E-mail: m.famulok@uni-bonn.de

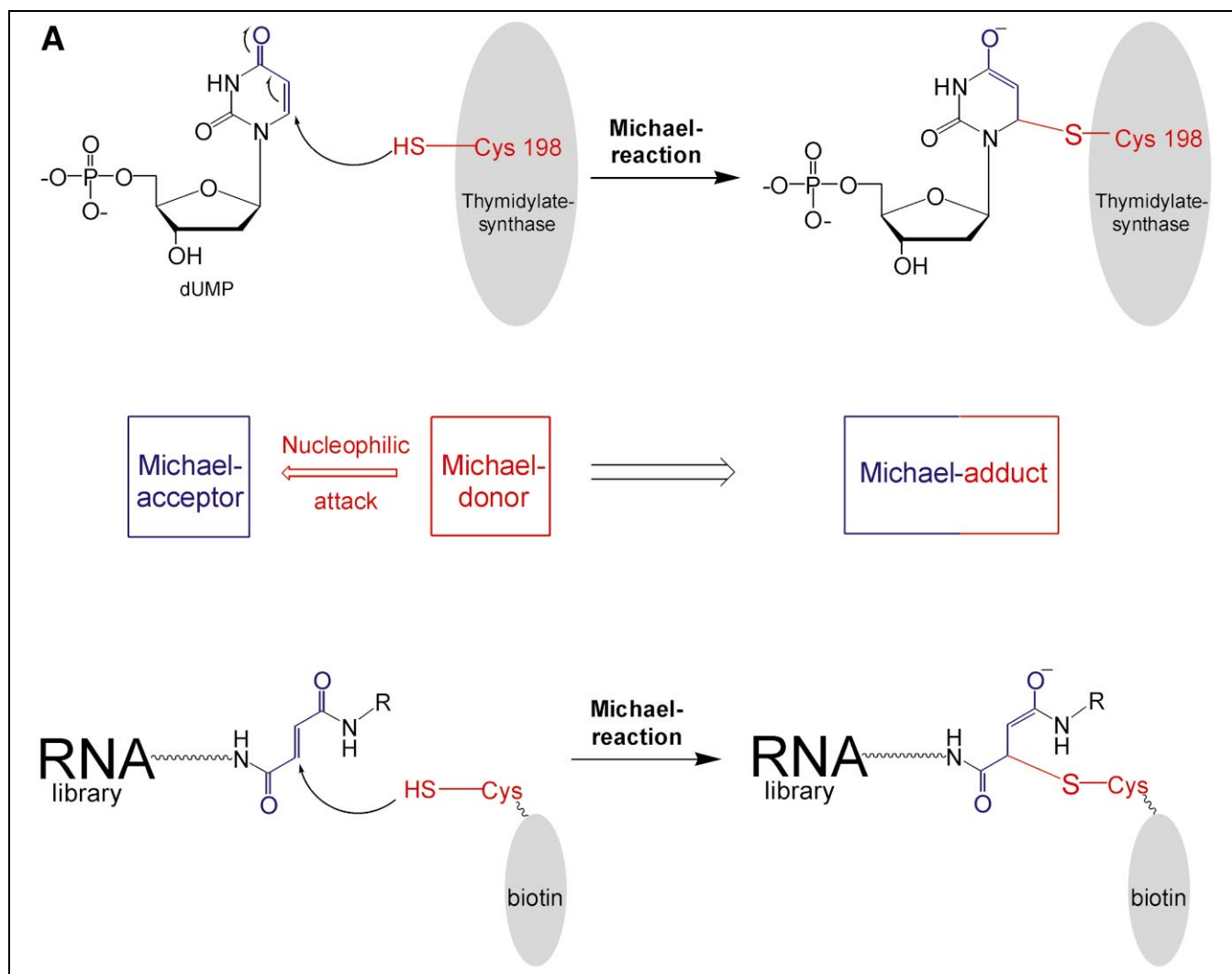


Fig. 1. (A) Schematic comparison of the Michael-addition activity of thymidylate synthase and the ribozyme activity. (B) Reaction step in the selection protocol for the Michaelase ribozymes. Catalytic RNA molecules in the fumaramide-derivatized library catalyze the formation of one S–C bond by nucleophilic attack of the free sulfhydryl group of the Michael-donor biotin cysteine (in red) to the unsaturated system of the Michael-acceptor fumaramide (in blue). Biotinylated product molecules are separated using streptavidin agarose. Immobilized RNAs are cleaved from the column by irradiation with UV-light and subjected to amplification. The photocleavable unit is indicated in pink.

scheme for generating RNA molecules with Michael-addition activity (Fig. 1). Our strategy involved generating a randomized pool of RNA conjugates in which a fumaramide moiety, a deactivated Michael-acceptor system, is covalently attached to each individual pool molecule via a flexible alkyl chain containing a photosensitive group. The resulting pool of fumaramide-derivatized RNA was then incubated with biotinylated cysteine as the Michael-donor to select RNA molecules that catalyze S–C bond formation between the two reactants. To avoid unintentional enrichment of catalysts that utilize other Michael-acceptor systems as reaction sites somewhere on the RNA molecule, we introduced a photosensitive group into the flexible linkage [20]. After removal of all non-biotinylated members of the pool by streptavidin agarose chromatography, only the desired catalysts could subsequently be

cleaved off the column by irradiation with UV-light in a highly specific manner.

2. Results

2.1. Library construction

We synthesized a pool of 2.0×10^{15} different RNA conjugates containing a total randomized region of 142 nt flanked by constant regions [21], containing an average of four copies of each species. The fumaramide moiety was attached to the 5'-end of the RNA molecules by transcription initiation with the fumaramide Michael-acceptor **1** as the initiator nucleotide. The fumaramide Michael-acceptor consists of guanosine monophosphate, the photo-

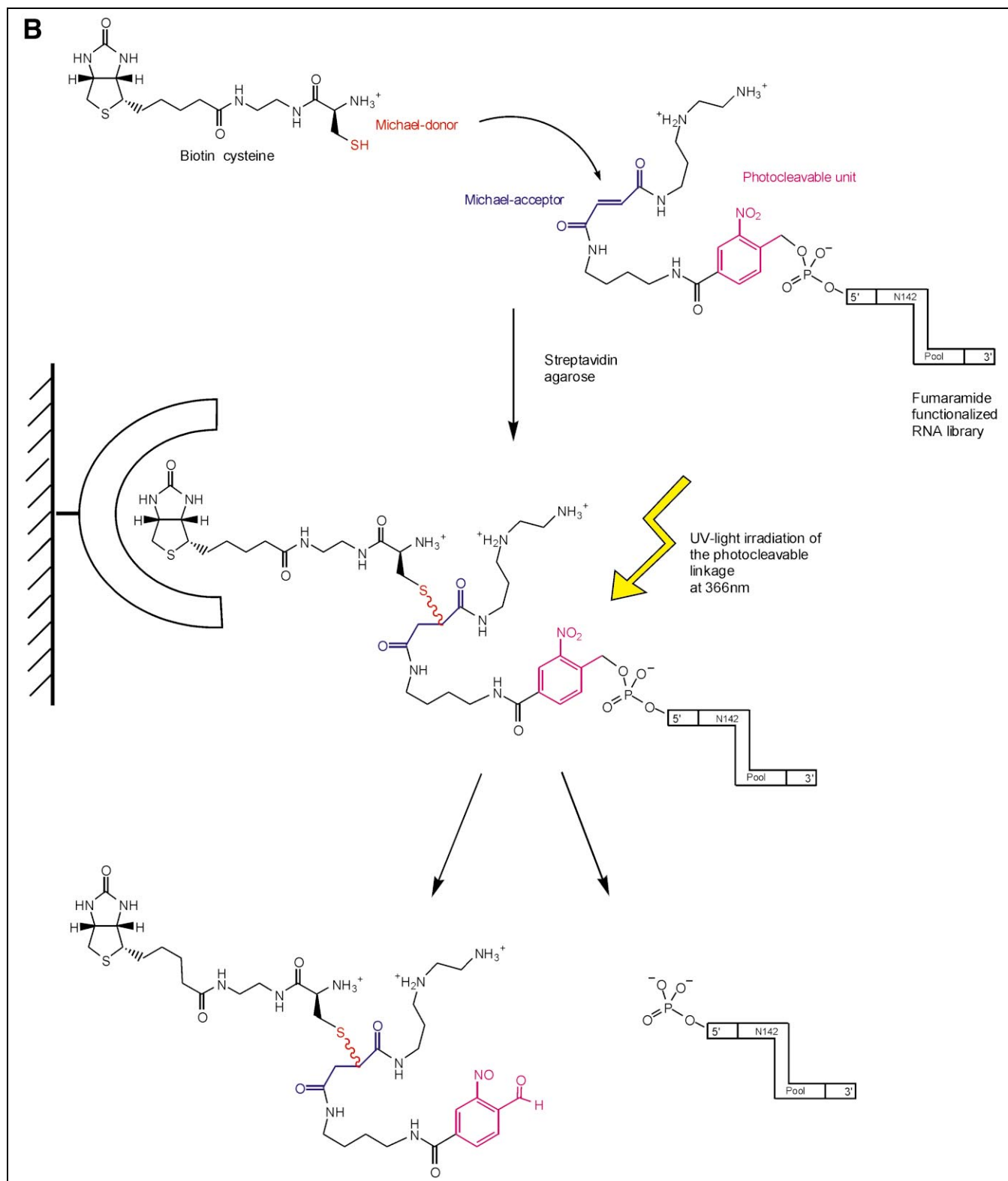


Fig. 1 (continued).

cleavable linkage and the fumaramide Michael-acceptor system. Under the applied conditions about 40% of the RNA transcripts were successfully primed (data not shown). After electrophoretic purification, the pool was used in the selection experiment.

2.2. Background reaction

To determine the rate of the uncatalyzed background reaction, unselected pool RNA molecules primed with the fumaramide-derivatized initiator nucleotide were pre-

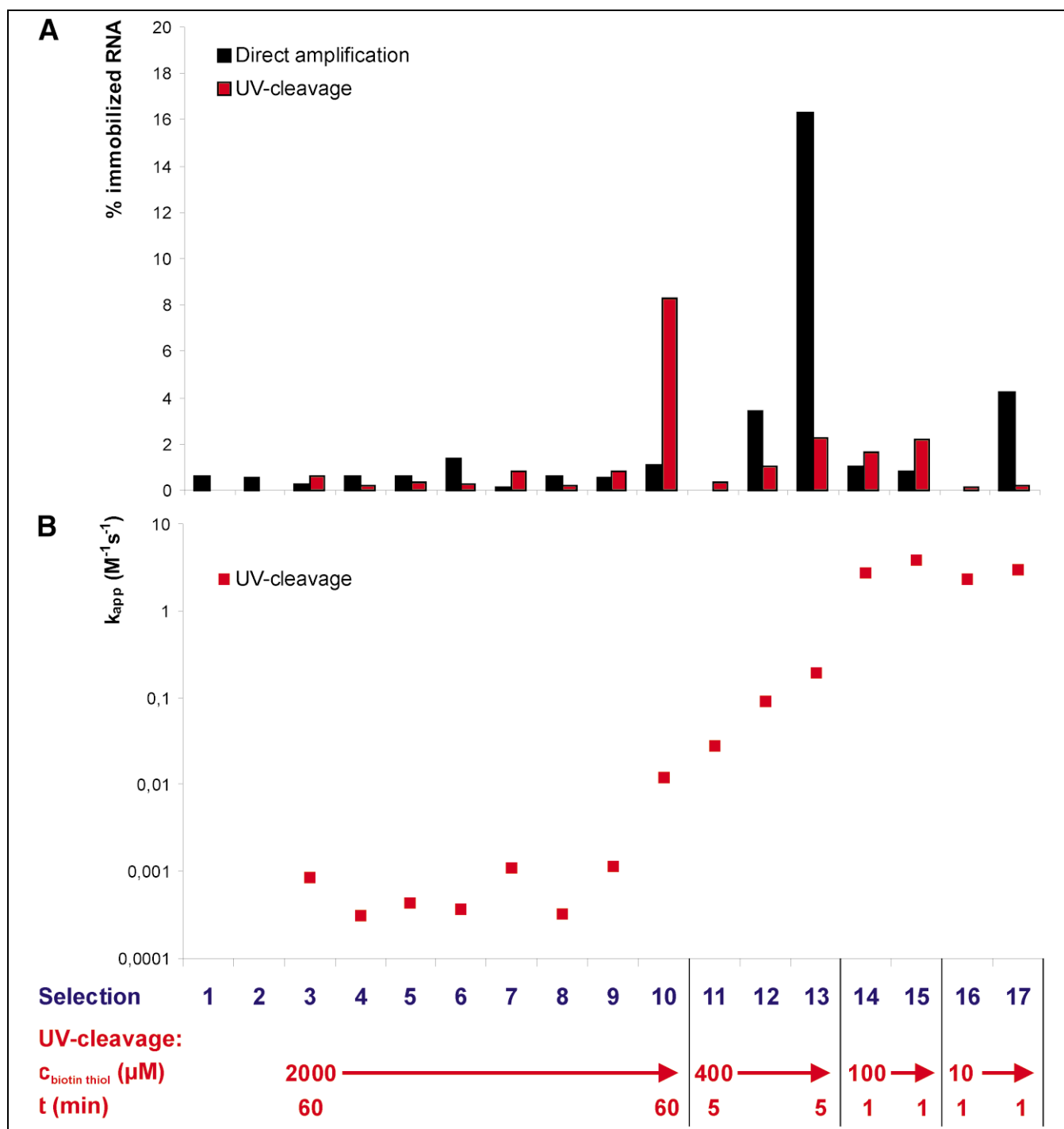


Fig. 2. Course of selection. (A) Enrichment of biotinylated RNA at each round of selection. Concentrations of biotin cysteine and reaction times are shown for each cycle. (B) Apparent rate constants of the UV-cleavage pool after each selection cycle. Concentrations of biotin cysteine and reaction times are shown for each cycle.

pared by T7 transcription, and incubated in the presence of increasing concentrations of biotinylated cysteine Michael-donor substrate ranging from 10 to 50 mM. Column affinity chromatography of the reaction mixtures revealed a value of k_{uncat} of $0.17 \pm 3 \times 10^{-3} M^{-1} h^{-1}$ (see Table 2) under the selection conditions. The unmodified RNA pool showed no background reaction, supporting the assump-

tion that the fumaramide moiety would be the only reaction site.

2.3. Selection

The introduction of the photocleavable linker proved to be useful for providing a highly specific elution of func-

tional RNAs by photoirradiation. Pilot experiments established that the cleavage efficiency of the photosensitive unit was quantitative in solution. However, when the RNA was immobilized on the streptavidin agarose resin, the efficiency of photocleavage was around 30%. As expected, no degradation of RNA molecules was detectable under the cleavage and incubation conditions. To avoid loss of functional molecules in the initial selection cycles due to sub-optimal photocleavage, we omitted the photocleavage step in the first two cycles and performed the amplification directly on the streptavidin resin. The photoirradiation step was introduced from cycle 3 onwards ('UV-cleavage' selection). In parallel, we continued the 'direct amplification' selection as a control and to compare both selection strategies with each other. In the first 10 cycles of the 'UV-cleavage' selection and in the first 12 cycles of the 'direct amplification' selection, 2 mM biotin cysteine was incubated with 1 μM fumaramide-RNA. The incubation time was 1 h, which would lead to 0.03% conversion due to the uncatalyzed background reaction.

In the first five rounds of both selections, between 0.2 and 0.6% of the library were continuously immobilized on streptavidin agarose. The background rate in the sixth round of the 'direct amplification' selection resulted in up to 1.37% immobilized RNA, which was likely due to slight enrichment of matrix binders. To prevent further enrichment of unspecific binders, we carried out a preselection against streptavidin agarose prior to the addition of cysteine biotin in every further round of both selections from round 7 onwards.

As a negative control, enriched libraries from each round of selection were transcribed without the fumaramide-initiator nucleotide. Incubation of these libraries

with the Michael-donor substrate resulted in less than 0.2% immobilized RNA for each pool tested. This result shows that priming with the initiator nucleotide is required for covalent attachment to the Michael-donor and suggests that the fumaramide moiety is the reaction site. In rounds 12–16 of the 'direct amplification' selection and cycles 10–14 of the 'UV-cleavage' selection, the selection pressure was gradually increased by shortening the incubation time from 1 h in the initial cycles to 1 min and reducing the concentration of the Michael-donor substrate from 2 mM to 100 μM.

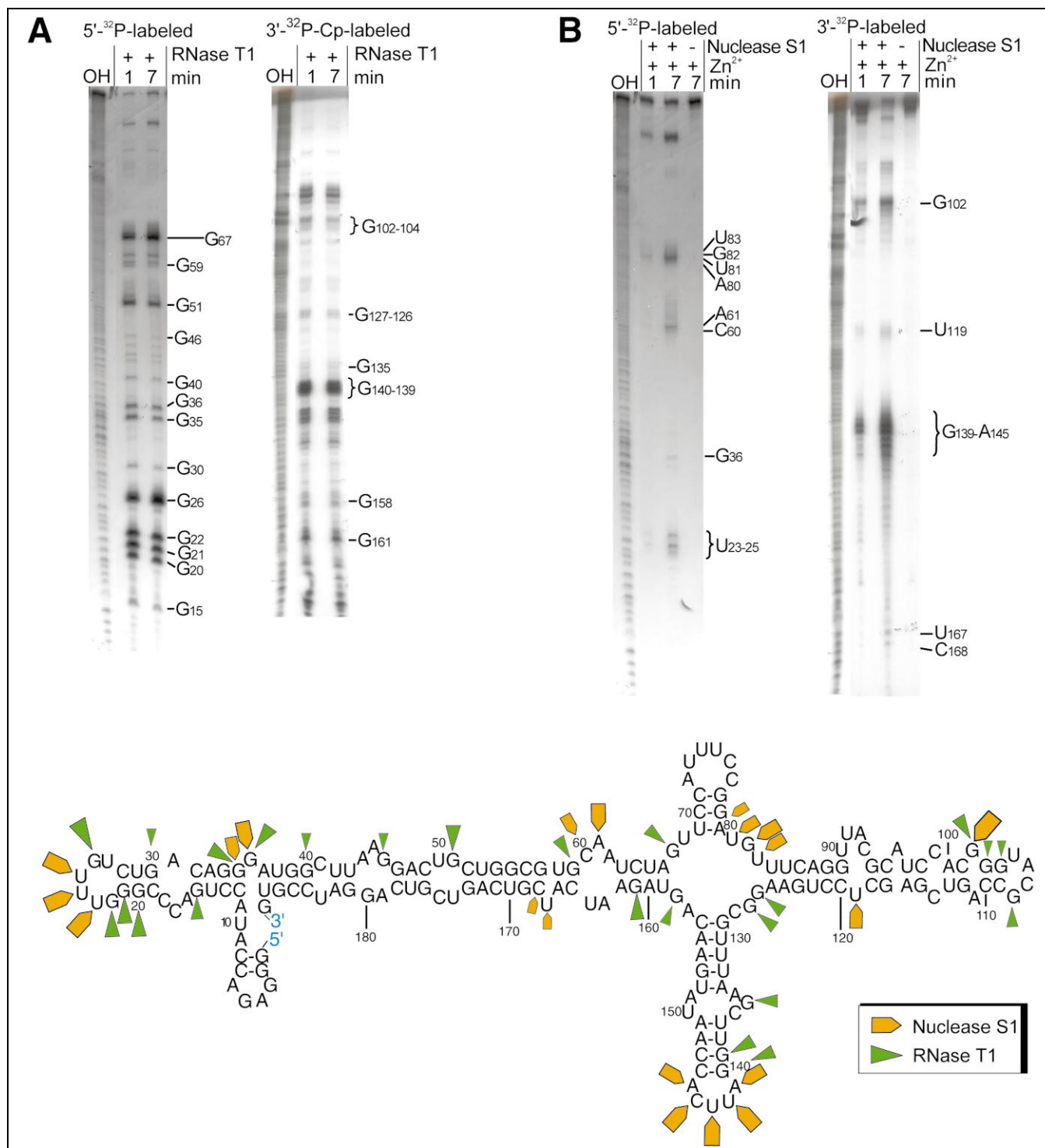
Fig. 2A directly compares the progress of both of these selections. Beginning with round 10 of the 'direct amplification' selection the percentage of immobilized RNA increased successively to up to 16.3% in round 12. In case of the 'UV-cleavage' selection, however, the fraction of immobilized RNA increased to 8.3% already in round 10, reflecting the more specific elution in this strategy. Fig. 2B shows that the apparent rate enhancement of the 'UV-cleavage' libraries gradually increased at each cycle of enrichment until a plateau was reached from cycle 14 onwards indicating that the selection had proceeded to maximal activity and that no further enrichment could be achieved despite increased selection stringency in cycles 16 and 17. Thus, the low level of photocleavage from the column was overcome by the more stringent selection strategy. Interestingly, however, the extent of cleavage efficiency gradually improved from 30% up to 80% in the course of the selection (data not shown).

2.4. Cloning and sequence analysis

Cloning and sequencing of 36 members of both final

Sequences of the "UV-cleavage"-selection:		$k_{obs}^{10^3}$ (min ⁻¹)
Clone		
UV		
1	CCGGGTTTGTCGACAGGGATGGCTTAAGGACTGCTGGCGAGCCAATCTAGTTCATTCCGATGTTTACGGGTACGCCAGTCGAGCTCCTGAAGGCGTTTAAAGCTTGGATTCACCAATATGACAGTAGA-TCATC	
2	CCGGGTTTGTCGACAGGGATGGCTTAAGGACTGCTGGCGAGCCAATCTAGTTCATTCCGGATGTTTACGGGTACGCCAGTCGAGCTCCTGAAGGCGTTTAAAGCTTGGATTCACCAATATGACAGTAGA-TCATC	
3	CCGGGTTTGTCGACAGGGATGGCTTAAGGACTGCTGGCGAGCCAATCTAGTTCATTCCGGATGTTTACGGGTACGCCAGTCGAGCTCCTGAAGGCGTTTAAAGCTTGGATTCACCAATATGACAGTAGAATCATC	
4	CCGGGTTTGTCGACAGGGATGGCTTAAGGACTGCTGGCGAGCCAATCTAGTTCATTCCGGATGTTTACGGGTACGCCAGTCGAGCTCCTGAAGGCGTTTAAAGCTTGGATTCACCAATATGACAGTAGAATCATC	
5	CCGGGTTTGTCGACAGGGATGGCTTAAGGACTGCTGGCGAGCCAATCTAGTTCATTCCGGATGTTTACGGGTACGCCAGTCGAGCTCCTGAAGGCGTTTAAAGCTTGGATTCACCAATATGACAGTAGAATCATC	38 ± 4
14	CCGGGTTTGTCGACAGGGATGGCTTAAGGACTGCTGGCGAGCCAATCTAGTTCATTCCGGATGTTTACGGGTACGCCAGTCGAGCTCCTGAAGGCGTTTAAAGCTTGGATTCACCAATATGACAGTAGAATCATC	
15	CCGGGTTTGTCGACAGGGATGGCTTAAGGACTGCTGGCGAGCCAATCTAGTTCATTCCGGATGTTTACGGGTACGCCAGTCGAGCTCCTGAAGGCGTTTAAAGCTTGGATTCACCAATATGACAGTAGAATCATC	
19	CCGGGTTTGTCGACAGGGATGGCTTAAGGACTGCTGGCGAGCCAATCTAGTTCATTCCGGATGTTTACGGGTACGCCAGTCGAGCTCCTGAAGGCGTTTAAAGCTTGGATTCACCAATATGACAGTAGAATCATC	
29	CCGGGTTTGTCGACAGGGATGGCTTAAGGACTGCTGGCGAGCCAATCTAGTTCATTCCGGATGTTTACGGGTACGCCAGTCGAGCTCCTGAAGGCGTTTAAAGCTTGGATTCACCAATATGACAGTAGAATCATC	
30	CCGGGTTTGTCGACAGGGATGGCTTAAGGACTGCTGGCGAGCCAATCTAGTTCATTCCGGATGTTTACGGGTACGCCAGTCGAGCTCCTGAAGGCGTTTAAAGCTTGGATTCACCAATATGACAGTAGAATCATC	37 ± 5
Sequences of the "direct-amplification"-selection:		
Clone		
SA		
2	CCGGGTTTTCGACAGGGATGGCTTAAGGACTGCTGGCGAGCCAATCTAGTTCATTCCGGATGTTTACGGGTACGCCAGTCGAGCTCCTGAAGGCGTTTAAAGCTTGGATTCACCAATATGACAGTAGAATCATC	
3	CCGGGTTTTCGACAGGGATGGCTTAAGGACTGCTGGCGAGCCAATCTAGTTCATTCCGGATGTTTACGGGTACGCCAGTCGAGCTCCTGAAGGCGTTTAAAGCTTGGATTCACCAATATGACAGTAGAATCATC	
17	CCGGGTTTTCGACAGGGATGGCTTAAGGACTGCTGGCGAGCCAATCTAGTTCATTCCGGATGTTTACGGGTACGCCAGTCGAGCTCCTGAAGGCGTTTAAAGCTTGGATTCACCAATATGACAGTAGAATCATC	37 ± 7
18	CCGGGTTTTCGACAGGGATGGCTTAAGGACTGCTGGCGAGCCAATCTAGTTCATTCCGGATGTTTACGGGTACGCCAGTCGAGCTCCTGAAGGCGTTTAAAGCTTGGATTCACCAATATGACAGTAGAATCATC	
19	CCGGGTTTTCGACAGGGATGGCTTAAGGACTGCTGGCGAGCCAATCTAGTTCATTCCGGATGTTTACGGGTACGCCAGTCGAGCTCCTGAAGGCGTTTAAAGCTTGGATTCACCAATATGACAGTAGAATCATC	
29	CCGGGTTTTCGACAGGGATGGCTTAAGGACTGCTGGCGAGCCAATCTAGTTCATTCCGGATGTTTACGGGTACGCCAGTCGAGCTCCTGAAGGCGTTTAAAGCTTGGATTCACCAATATGACAGTAGAATCATC	
30	CCGGGTTTTCGACAGGGATGGCTTAAGGACTGCTGGCGAGCCAATCTAGTTCATTCCGGATGTTTACGGGTACGCCAGTCGAGCTCCTGAAGGCGTTTAAAGCTTGGATTCACCAATATGACAGTAGAATCATC	
26	CCGGGTTTTCGACAGGGATGGCTTAAGGACTGCTGGCGAGCCAATCTAGTTCATTCCGGATGTTTACGGGTACGCCAGTCGAGCTCCTGAAGGCGTTTAAAGCTTGGATTCACCAATATGACAGTAGAATCATC	36 ± 3
32	CCGGGTTTTCGACAGGGATGGCTTAAGGACTGCTGGCGAGCCAATCTAGTTCATTCCGGATGTTTACGGGTACGCCAGTCGAGCTCCTGAAGGCGTTTAAAGCTTGGATTCACCAATATGACAGTAGAATCATC	
33	CCGGGTTTTCGACAGGGATGGCTTAAGGACTGCTGGCGAGCCAATCTAGTTCATTCCGGATGTTTACGGGTACGCCAGTCGAGCTCCTGAAGGCGTTTAAAGCTTGGATTCACCAATATGACAGTAGAATCATC	
4	GTACGCCCGGGTCTGCTGCATTCCAGTAGCTAGGTTTCCGGCTTCCAAAGTCTATTCCTCAGGTCAGAGTCCACAAGTCTCATCGCCATATACTCGTTCCAGGTTACTGCTCTCAGCTC	0.02 ± 0.002
20	TGCTACCGGGTCTATATCTCGTTTCCATGTCCTACTATGCGCGATGGTTCGCTAGGTTTATGATGTTGATTGCGAGTCAGTCGCGAAACCTCAGTGCATTGACAACATTGC	0.08 ± 0.004

Fig. 3. Sequences of the selected clones. Only sequences from randomized regions are given. Mutations or deletions within the clone sequences are shown in bold. Orphan sequences (SA 4, SA 20) were only found in the 'direct amplification' selection. For comparison, the values of k_{obs} (min⁻¹) of selection pool UV10 = $2.3 \times 10^{-4} \pm 0.3 \times 10^{-4}$, pool UV14 = $29 \times 10^{-3} \pm 5 \times 10^{-3}$, pool SA12 = $4.0 \times 10^{-4} \pm 0.5 \times 10^{-4}$, pool SA16 = $25 \times 10^{-3} \pm 7 \times 10^{-3}$.



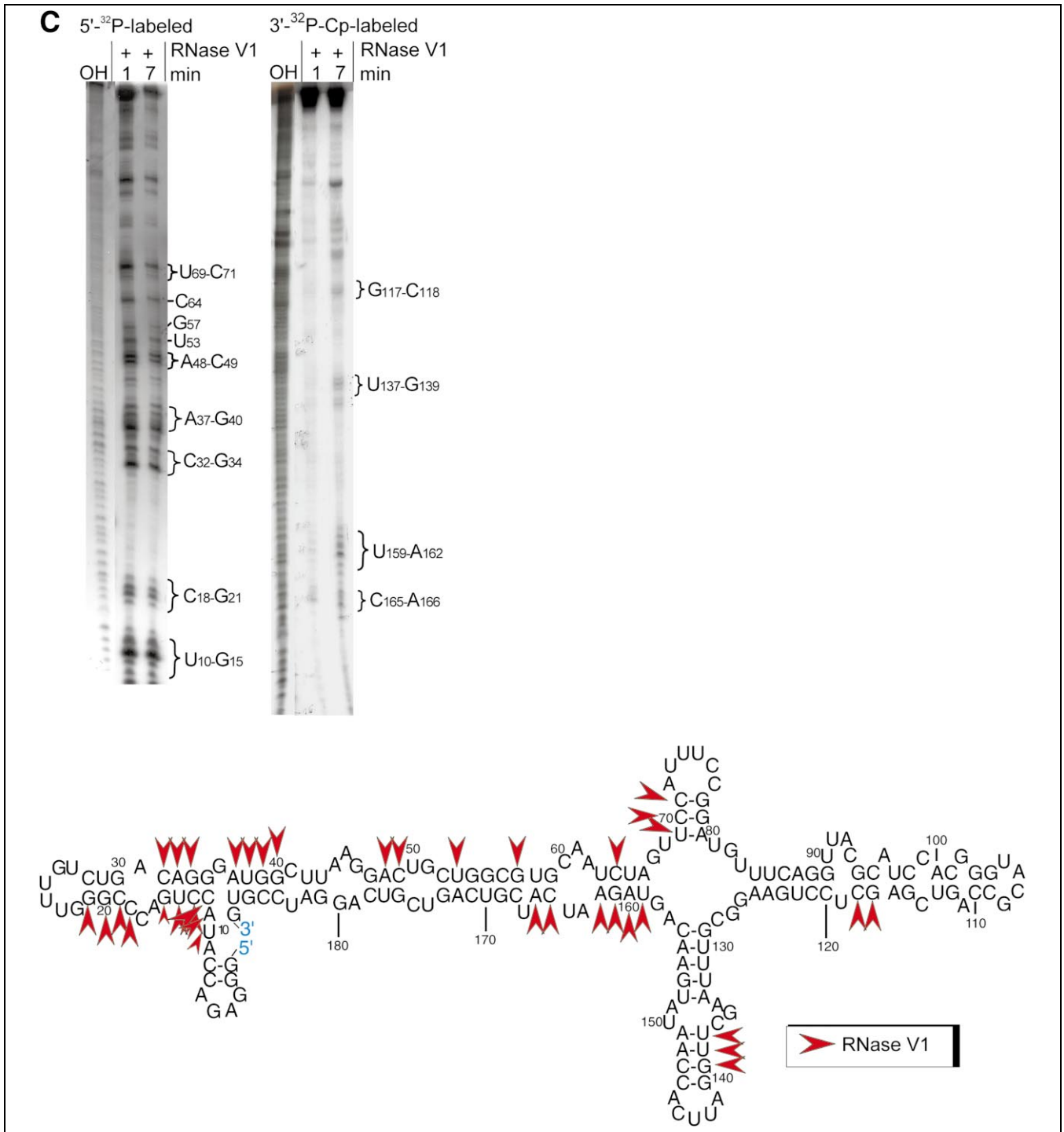


Fig. 4 (continued).

ciency. These results indicate that improvement of catalytic activity was the major selection criterion in both selections. The gradual increase of cleavage activity in case of the ‘UV-cleavage’ selection (Fig. 2), obviously does not reflect any overlaying selection criterion.

Fig. 4 shows the proposed secondary structure of clone UV5 RNA based on a thermodynamic folding algorithm [22]. This secondary structure prediction was supported by enzymatic probing using structure or base-specific ribonu-

cleases T1, S1, and V1. To examine the minimal sequence requirements for catalytic activity, we carried out a deletion analysis of a single clone, UV5, by construction of truncated versions of the ribozyme. This was achieved by nested PCR amplification of the DNA using combinations of appropriate primers, followed by in vitro transcription. Table 1 summarizes the activity of the tested constructs in the presence of 12 mM Mg²⁺. Deletion of the first 17 nucleotides of clone UV5, which is the entire 5'-primer

Table 1

Comparison of the intramolecular Michael-addition rates of truncated clone UV5 variants

Clone UV5 construct (nucleotide position)	$k_{\text{obs}} \times 10^{-3}$ (min^{-1}) ^a
1–188	7.7 ± 0.2
1–168	4.5 ± 0.3
1–148	4.3 ± 0.1
1–128	n.d. ^b
1–108	0
1–88	0
1–68	0
1–48	0
17–188	0
37–188	0

^aReaction conditions: 1 μM ribozyme was incubated with 1 mM **1** at room temperature in selection buffer containing 12 mM MgCl_2 . Aliquots were taken at different time points and coupled to streptavidin agarose. First order rate constants were obtained from the data by fitting the equation $[\text{P}]_t = [\text{RNA}] - [\text{RNA}] \exp(-k_{\text{obs}} t)$, where $[\text{P}]_t$ is the concentration of biotinylated RNA and $[\text{RNA}]$ is the concentration of fumaramide derivatized clone UV5.

^bThe reaction was too slow to calculate k_{obs} . The length of all RNAs was confirmed by PAGE.

binding site, results in complete loss of activity, whereas deletion of the 40 3'-terminal bases resulted in reduction of activity by a factor of 1.8.

2.5. Clone UV5 is a Michaelase

We next investigated whether the catalyzed reaction indeed occurred at the carbon–carbon double bond of the fumaramide moiety of the deactivated Michael-acceptor. For that we performed a negative control experiment using a newly synthesized initiator nucleotide **4** (Fig. 5) in which the double bond of the fumaramide was replaced by a single bond. **4** was used for 5'-priming of UV5. Kinetic measurements performed with this reduced form of UV5 showed no detectable reactivity indicating that the carbon–carbon double bond of the fumaramide moiety of

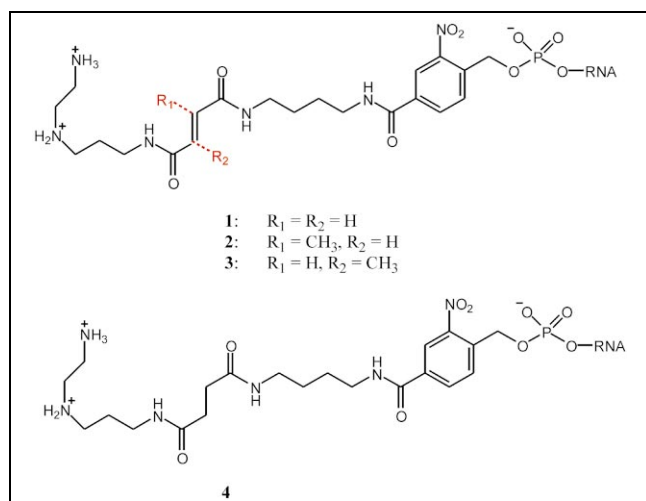


Fig. 5. Synthesized derivatives **2**, **3**, **4** of the fumaramide substrate **1**.

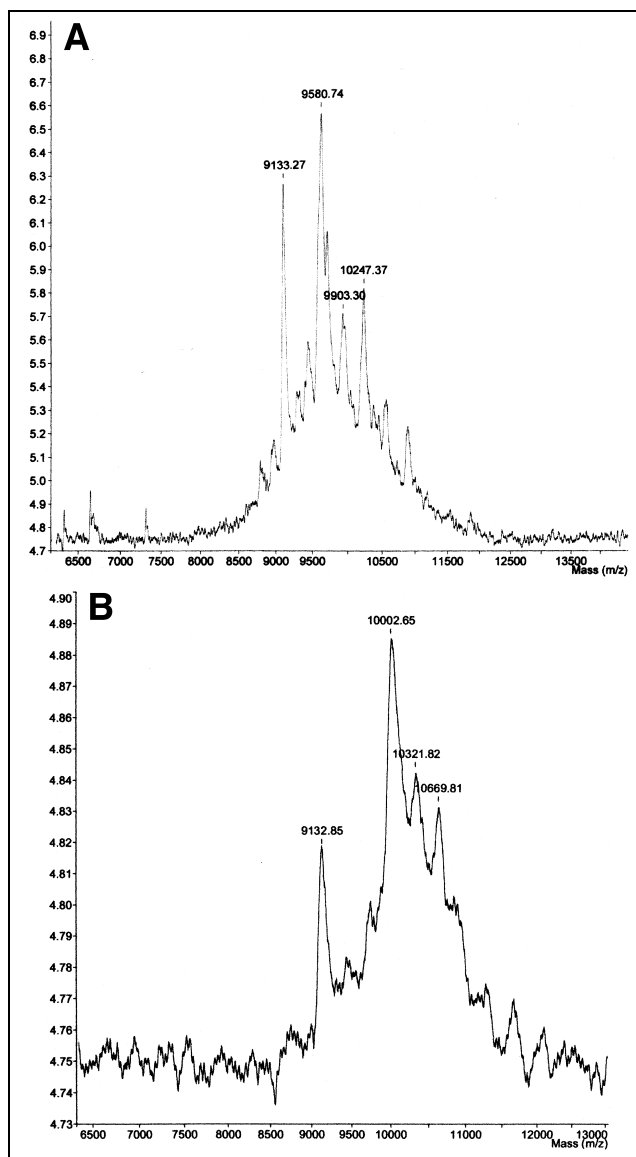


Fig. 6. MALDI-TOF analysis of primed ribozyme UV5 RNA after RNase H digest. (A) Representative MALDI-TOF analysis of the primed short cleavage products. The calculated molecular weights (av.) of the G-fuma primed RNA 28-, 29- and 30-mers are 9582.01 Da ($[\text{M}+\text{H}]^+$), found 9580.74; 9902.22 Da ($[\text{M}+\text{H}]^+$), found 9903.30 and 10247.44 Da ($[\text{M}+\text{H}]^+$), found 10247.37. The peak found at 9133.27 Da ($[\text{M}+\text{H}]^+$) (calculated: 9134.78) is representing the portion of cleaving product of the primed RNA 28-mer, where the photosensitive fumaramide linkage was cleaved off induced by the laser light of the spectrometer at 337 nm. (B) Representative MALDI-TOF analysis of short RNA-Michael-adduct 28-, 29- and 30-mers formed by RNase H digest of UV5 ribozyme RNA carrying the biotin cysteine-fumaramide Michael-adduct. The calculated molecular weights (av.) of the Michael-adduct RNA 28-, 29- and 30-mers are 10003.23 Da ($[\text{M}+\text{H}]^+$), found 10002.65; 10323.44 Da ($[\text{M}+\text{H}]^+$), found 10321.82 and 10668.66 Da ($[\text{M}+\text{H}]^+$), found 10669.81. Similar to (B) there is also a peak found at 9132.85 Da ($[\text{M}+\text{H}]^+$) (calculated: 9134.78) representing the portion of photocleaved RNA-Michael-adduct 28-mer.

G-fuma (**1**) is the exclusive site for the nucleophilic attack of the sulfhydryl group of the biotin cysteine Michael-donor substrate.

In order to determine the increase of molecular weight

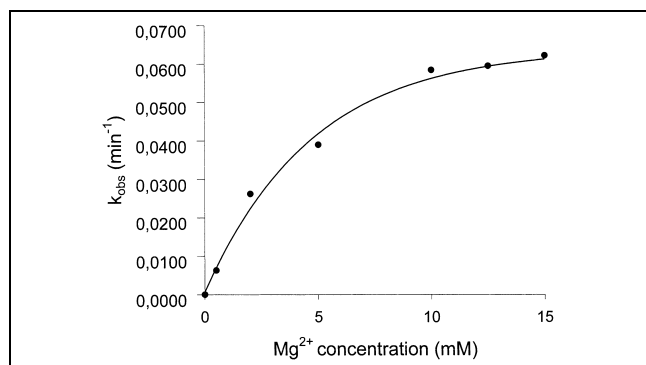


Fig. 7. The ribozyme activity is dependent on Mg^{2+} . The reactions were performed at room temperature at a concentration of $1 \mu M$ of radiolabeled clone UV5 RNA and 0.5 mM biotin cysteine in selection buffer (50 mM K-MOPS, pH 7.4, 200 mM NaCl). Observed rate constant values were obtained by affinity chromatography after coupling the biotinylated RNA to a streptavidin agarose matrix.

of ribozyme UV5 RNA as a result of formation of the biotin cysteine-fumaramide Michael-adduct, a MALDI-TOF analysis was carried out. Because of the molecular weight of $> 62 \text{ kDa}$ of the 188 nt long ribozyme motif, the theoretical difference between the unreacted and reacted ribozyme molecule of 0.42 kDa lies within the error range of the technical equipment and thus cannot be reliably measured. Therefore, to determine the exact differences in mass between reacted and unreacted ribozyme RNA, we performed RNase H digestions to cut off a small RNA oligomer of defined length, comprising the first 20–40 nucleotides of the ribozyme including its modified 5'-end. The site of digestion was determined by hybridization with short DNA oligonucleotides which form RNA•DNA hybrids at nucleotide positions 20–40, 20 nucleotides downstream of the 5'-end of the ribozyme UV5 RNA. Fumaramide-derivatized and reacted Michael-adduct ribozyme RNA was digested with RNase H in that way and subjected to MALDI-TOF analysis. The spectrum (see Fig. 6A) shows one major peak at 9580.74 Da representing the fumaramide-RNA 28-mer and two peaks of lower intensity at 9903.30 Da and 10247.37 Da , representing the derivatized RNA 29- and 30-mer. The peak found at 9133.27 Da represents the portion of the major peak (28-mer) at 9580.74 Da , where the photosensitive fumaramide linkage was cleaved off induced by the laser light of the MALDI-TOF spectrometer at 337 nm .

For comparison, we carried out the same MALDI-TOF analysis using the corresponding short 28, 29- and 30-mers derived from reacted Michael-adduct RNA, additionally carrying the biotinylated cysteine (Fig. 6B). For this purpose, the short biotinylated RNA cleavage products were isolated and purified by affinity chromatography using their biotin affinity tag. The immobilized RNA fraction was eluted by mercaptoethanol-elution [23] and prepared for MALDI-TOF analysis. Similar to the spectrum shown in Fig. 6A we also found a peak at 9132.85 Da representing the photocleaved portion of the Michael-adduct RNA

28-mer. The deviation of all determined mass values from their calculated values is less than 2 Da , which is within the error range of the expected values.

The calculation of the difference of the mass data between the Michael-adduct RNA oligomers and the non-reacted fumaramide-RNA oligomers gives an average of $420.95 \pm 1.74 \text{ Da}$ ($\Delta_{\text{theoretical}} = 420.21 \text{ Da}$). This analysis confirmed that ribozyme UV5 catalyzes the transfer of the biotin cysteine to the fumaramide linkage substrate and provides further evidence that a Michael-addition reaction is catalyzed.

2.6. Kinetic characterization and salt dependence of the UV5 ribozyme

The Mg^{2+} dependence of the observed rate constant shows a hyperbolic profile (Fig. 7). At 15 mM Mg^{2+} the k_{obs} reached a plateau of 0.0623 min^{-1} whereas no detectable enzymatic activity was measured in the absence of Mg^{2+} . Higher Mg^{2+} concentrations led to aggregation and precipitation of the RNA. The same rate acceleration as obtained with 5 mM Mg^{2+} was also found with 5 mM Mn^{2+} . Replacement of 5 mM Mg^{2+} with 5 mM Ca^{2+} resulted in a 25% reduction of activity. The monovalent cations were also exchangeable. The exchange of 200 mM Na^{+} with 200 mM K^{+} in the selection buffer gave exactly the same rate accelerations determined under selection conditions. Kinetic analyses of the self-modification reaction were performed in the range of $50\text{--}1000 \mu M$ of biotin cysteine following Michaelis–Menten kinetics, with a K_m

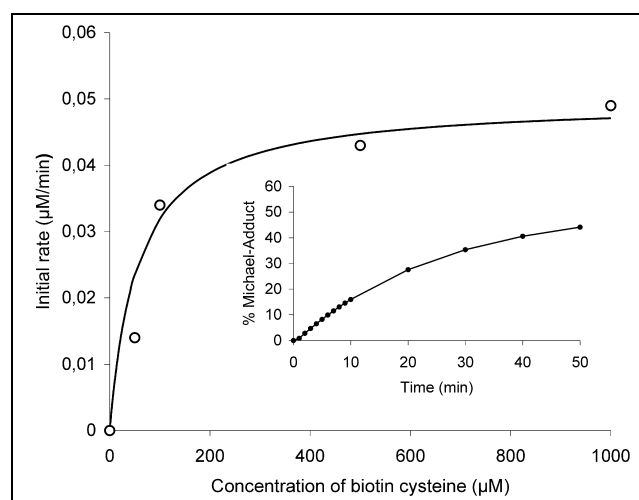


Fig. 8. Characterization of the intramolecular reaction catalyzed by clone UV5. Initial rates v_0 are plotted against biotin cysteine concentrations ranging from $50 \mu M$ to 1 mM . Values of the Michaelis–Menten parameters K_m and k_{cat} were obtained from the data fitting the equation $v_0 = [RNA]_0 [biotin \text{ cysteine}] k_{\text{cat}} / (K_m + [biotin \text{ cysteine}])$ using Kaleidagraph (Abelbeck Software). Inset: curve fitting of the Michaelase reaction using $1 \mu M$ clone UV5 RNA and $250 \mu M$ biotin cysteine. Rate constants k_{obs} were calculated from the equation $[P]_t = [RNA] - [RNA] \exp(-k_{\text{obs}} t)$, where $[P]_t$ is the concentration of biotinylated RNA at time t and $[RNA]$ is the concentration of clone UV5 RNA.

Table 2
Specificity of the Michaelase ribozyme UV5

Kinetic parameters ^a	1	2	3
k_{uncat} ($\text{M}^{-1} \text{h}^{-1}$)	$0.17 \pm 3 \times 10^{-3}$	$0.13 \pm 5 \times 10^{-3}$	$0.16 \pm 4 \times 10^{-3}$
k_{cat} (min^{-1})	$0.05 \pm 2 \times 10^{-3}$	$0.03 \pm 1 \times 10^{-3}$	$0.03 \pm 2 \times 10^{-3}$
K_{M} (μM)	56 ± 9	300 ± 66	571 ± 82
$k_{\text{cat}}/K_{\text{M}}$ ($\text{M}^{-1} \text{h}^{-1}$)	53 300	6 400	2 800
rate enhancement	3.0×10^5	4.9×10^4	1.8×10^4

The kinetic parameters of the ribozyme UV5 primed with Michael-acceptor substrates **2**, and **3**, compared to UV5 primed with the non-derivatized substrate **1**.

^aWith k_{uncat} : apparent background second-order rate constant, k_{cat} : first-order rate constant for catalysis, K_{M} : substrate concentration [biotin cysteine] at which half-maximal reaction is achieved, $k_{\text{cat}}/K_{\text{M}}$: specificity constant for substrate recognition, rate enhancement: $(k_{\text{cat}}/K_{\text{M}})/k_{\text{uncat}}$.

of $56 \pm 9 \mu\text{M}$ and a k_{cat} of $0.05 \pm 2 \times 10^{-3} \text{ min}^{-1}$ in the presence of 5 mM Mg^{2+} (Fig. 8). With a $k_{\text{cat}}/K_{\text{m}}$ of $888 \text{ M}^{-1} \text{ min}^{-1}$ the ribozyme is showing a rate enhancement of 3.0×10^5 over the uncatalyzed reaction (see Table 2).

2.7. *In trans* reaction

To study whether clone UV5 acts as a true catalyst, we incubated clone UV5 and a variant of clone UV5 RNA, lacking the first G-nucleotide, with various ratios of the two substrates in solution. There was, however, no detectable rate acceleration under these conditions. We then prepared a truncated 168-mer ribozyme (UV5, 20–188) lacking the first 20 nucleotides from the 5'-end. The 5'-derivatized RNA 20-mer substrate was prepared by *in vitro* T7-transcription of the encoding DNA template. The *trans* reaction was performed under single-turnover conditions. Aliquots withdrawn at the specified time points were analyzed using denaturing polyacrylamide gel electrophoresis (PAGE). Fig. 9 shows the reaction of the fumaramide-derivatized RNA 20-mer transcript with biotin cysteine catalyzed by UV5, 20–188 at a concentration of 5 mM MgCl_2 at ambient temperature (23°C). From the ratio of the bands, k_{obs} was calculated to be $0,058 \text{ min}^{-1}$, which corresponds to a more than 5000-fold rate acceleration under these conditions. However, under multiple turnover conditions no $k_{\text{cat}}/K_{\text{m}}$ could be determined, presumably due to the fact that the dissociation of the RNA 20-mer oligonucleotide substrate is very slow. The biotinylated oligonucleotide substrate pairs

over an extended region with the enzyme so that its dissociation becomes rate-limiting for the forward reaction. Currently we are trying to engineer the substrate oligonucleotide to have an increased rate of dissociation for the ribozyme/oligonucleotide substrate complex, to facilitate the determination of $k_{\text{cat}}/K_{\text{m}}$ under multiple turnover conditions.

2.8. Mechanistic investigations

To gain insight into the specificity and molecular aspects of substrate recognition, we performed inhibition and competition studies using fragments of biotin cysteine (Fig. 10). In presence of a 100-fold excess of cysteine and acyl diamidoethyl-cysteine over the biotin cysteine Michael-donor substrate the reaction appeared to be unaffected, whereas biotin was found to act as a competitive inhibitor with a K_i of $5.7 \pm 0.8 \text{ mM}$. These results suggest that the biotin group participates in the molecular recognition of the biotinylated substrate to a large extent. Thereby, the UV5 RNA would represent a second example of a biotin-binding RNA catalyst that adds to a previously identified biotin-binding RNA pseudoknot structure [24].

We next investigated whether the ribozyme shows selectivity for one of the two possible carbon positions at the Michael-acceptor double bond. Both positions are equally suited as potential sites for the nucleophilic attack of the Michael-donor substrate. To address this issue, two derivatives of the fumaramide-tethered initiator nucleotide (**2**, **3**, see Fig. 5) in which either of the two hydrogen atoms of

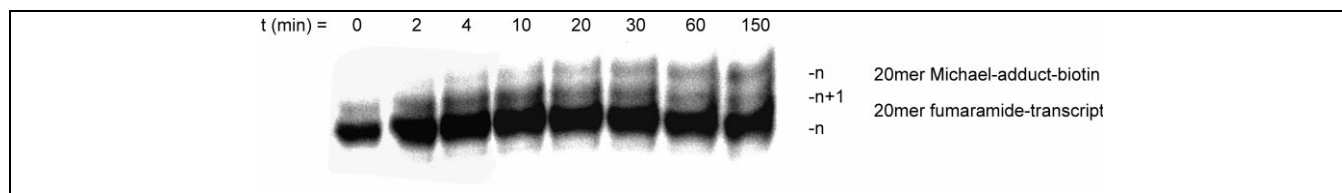


Fig. 9. Catalysis of the intermolecular reaction under single-turnover conditions. Reactions were performed in $1 \times$ selection buffer containing 200 mM NaCl , 5 mM MgCl_2 and 50 mM K-MOPS at $\text{pH } 7.4$. The concentration of the 20-mer fumaramide substrate was 4 nM , of the biotin cysteine 2.5 mM and of the ribozyme UV5, 20–188 $0.4 \mu\text{M}$. Aliquots were withdrawn at the indicated time points and reactions stopped by mixing with the same volume of stop solution (9 M urea , 20 mM EDTA , $\text{pH } 8.0$) and freezing to -80°C . Samples were analyzed on a denaturing 20% polyacrylamide gel and quantified on a phosphorimager.

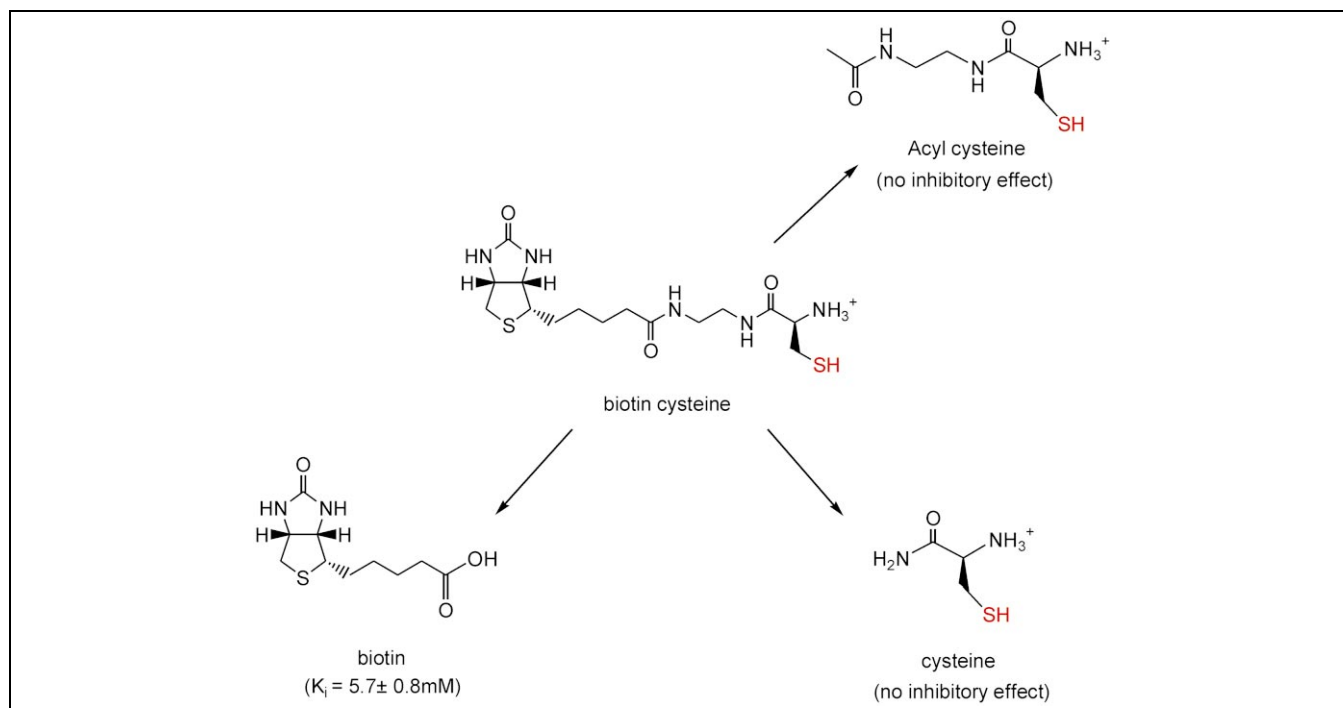


Fig. 10. Inhibition and competition studies of catalysis of clone UV5 with fragments and derivatives of biotin cysteine.

the C–C double bond was substituted by a methyl group were synthesized and used as initiator nucleotides to prime clone UV5. Kinetic characterization of the catalyzed reactions was performed in the range of 1–10 mM of biotin-substrate under the same conditions as for the RNA primed with the unsubstituted fumaramide substrate (**1**). Compared to the original fumaramide, the value of k_{cat}/K_m was reduced in the case of **2** and **3** by a factor of 8 and 19, respectively, and the corresponding rate enhancement was reduced by a factor of 6 and 16, respectively (Table 2). This change in the catalytic efficiency is largely determined by the marked differences in the K_M values for the different Michael-acceptor substrates (Table 2). While the values of K_M were enhanced by a factor of five for **2** and 10 for **3** (both compared to **1**), the values of k_{cat} and k_{uncat} , however, were only slightly changed for **1**, **2** and **3**, indicating only a marginal difference in reactivity due to the methyl-substitutions. These data provide strong evidence that the ribozyme UV5 forms a well-defined binding pocket for the covalently attached Michael-acceptor substrate that responds to differences in the methyl-substitution pattern and suggests that UV5 may also be capable of mediating the Michael-addition reaction in a regioselective manner. On the other hand, the fact that **2** and **3** show a k_{cat} that is about half of that of **1** could suggest that both ends of the alkene react with equal rates in **1**, but that methylation of either end shuts off the nucleophilic attack at that position for steric reasons. Alternatively, the methyl group may also serve to stabilize the intermediate ‘enolate’ leading to attack of the non-methylated end. The difference in the K_M values could then reflect the poorer fit

of the methylated compounds in a pocket that has been selected to bind the non-methylated compound. In this case, the ribozyme would not be regioselective at the non-methylated substrate.

3. Discussion

The ribozyme presented here is the first example of a Michaelase ribozyme isolated by *in vitro* selection. It requires a certain concentration of monovalent and divalent metal ions, but it can perform as well in the presence of a variety of different metal ions. This property makes the ribozyme functional under very different ‘environmental’ conditions.

We specifically chose the Michael reaction for the ribozyme selection, because it plays an important role in a number of biological reactions, but also represents one of the most important reactions in synthetic organic chemistry. The new RNA catalysts described here contribute interesting aspects to both fields of research by further supporting that complex metabolic transformations were catalyzed by RNA which may help to understand how prebiotic life could be linked to the modern protein–nucleic acid world. Using direct selection with linker-coupled reactants, we isolated a ribozyme that performs a Michael-addition reaction similar to that of the thymidylate synthase enzyme, i.e. the formation of a Michael-adduct by the nucleophilic addition of a cysteine to a deactivated α -, β -unsaturated Michael-acceptor system. Although direct selection had been applied to numerous self-modifying re-

actions for several years, its extension to reactions involving two non-RNA reactants has been reported recently [25–27]. In this study we successfully applied photocleavable linker molecules for in vitro selection protocols for the first time. It is shown that the application of cleavable linkers allows for a highly stringent selection protocol enforcing the enrichment of the desired activity. Although in both selections only one sequence dominated the final pools, the UV-cleavage selection proceeded with fewer cycles than the direct amplification selection. Point mutations inside the common sequence probably stem from misincorporations during the enzymatic amplification step.

Studies with various derivatives of both the Michael-donor and acceptor substrates indicate that the ribozyme has evolved specific binding pockets for both substrates. Inhibition studies performed with fragments comprising Michael-donor derivatives, cysteine, acyl cysteine and biotin, suggest that the substrate as a whole is recognized by the ribozyme whereby the biotinyl moiety contributes to the molecular recognition more than the cysteyle moiety. Thereby, the Michaelase described here represents a second example of an RNA catalyst that takes advantage of the biotin group as a ‘handle’ for the positioning of functional groups in the active site [28]. The fact that two separate RNA catalysts now seem to be capable of recognizing the biotin moiety and performing chemical transformations with functional groups appended to it may be supportive of theories suggesting that biotin might have played an important role as a frequently utilized RNA world cofactor [29].

Experiments using methylated derivatives of the linker-coupled substrate showed that the ribozyme possesses also high specificity for the fumaramide Michael-acceptor substrate. The substitution of only one hydrogen atom by a methyl group at either of the two possible positions of the double bond results in a 6–10-fold increase of the Michaelis–Menten constant, while the k_{cat} values remained largely unchanged. A possible explanation for this result would be that the ribozyme folds into a highly specific binding pocket where both substrates are positioned in a conformation in which the reaction can occur. The difference in catalytic efficiency depending on the position of the methyl group substitution suggests that the ribozyme shows aspects of regioselectivity. However, it is also possible that the attacking cysteine-thiol is positioned in the general vicinity of the double bond and can attack at either end. Methylation at one end or the other shuts down attack at that position.

The ribozyme could be engineered to transfer the Michael-donor substrate onto an external RNA oligonucleotide comprising the first 20 nt of the 5'-end. This is promising with regard to a further engineering of the Michaelase ribozyme aiming at the acceleration of the reaction between two free reactants. Such activities may lead to sequences which could potentially be used as helpful tools in organic synthesis.

4. Significance

The selection of catalysts by in vitro selection techniques allows incorporation of functional groups that have been proven to be important for catalysis in organic synthesis. We have demonstrated that ribozymes with Michael-addition activity similar to that of the thymidylate synthase can be directly evolved by in vitro selection. Consequently our isolated Michaelase ribozyme represents an example of a selected RNA catalyst for a central organic reaction. The ribozyme exhibits substrate specificity as it discriminates between derivatives with different methyl-substitutions at the Michael-acceptor double bond reaction site. By employing an external 20-mer oligonucleotide substrate and a truncated version of the catalytic RNA we showed that it also catalyzes the Michael reaction in trans. The Michaelase ribozyme exhibits a broad tolerance for different metal ions, making it functional under different salt conditions. In this system, catalysis of a complex reaction involving the creation of two bonds that requires exact positioning of the two reactants in the catalytic site is achieved by a ribozyme. The catalytic activity described here reveals the potential of ribozymes for performing comprehensive organic transformations, which are essential not only for recreating prebiotic reaction pathways but also for the application of RNA catalysts in bioorganic synthesis.

5. Materials and methods

5.1. Materials

T7 RNA polymerase and T4 polynucleotide kinase was purchased from Stratagene, [γ - ^{32}P]ATP, [α - ^{32}P]GTP, [$5'$ - ^{32}P]pCp from NEN, DNase I (RNase-free) from Roche, SuperScript II RNase H⁻ reverse transcriptase from Gibco, *Taq* polymerase from Eurogentec, RNase H was from Promega, RNase T1, RNase VI, Nuklease S1 from Amersham Pharmacia Biotech and T4 RNA ligase, calf intestinal alkaline phosphatase from New England Biolabs. Unlabelled NTPs and tRNA were obtained from Roche and dNTPs from Aldrich. Primers and synthetic oligonucleotides were either synthesized on a Millipore Expedite synthesizer using standard phosphoramidite chemistry or purchased from Metabion. Streptavidin agarose was purchased from Pierce, biotin from Aldrich. Spin filters (Ultrafree-MC 0.45 μm) were from Millipore. The synthesis of the Fumaramide–guanosine conjugate (initiator nucleotide) and of its saturated and methylated derivatives 1–4 as well as of the biotinylated cysteine substrate will be described elsewhere.

5.2. Preparation of the RNA pool

The oligonucleotides PM1, 5'-AGC GAA TTC TAA TAC GAC TCA CTA TAG GGA GAG CCA TAC CTG AC-3'; PM2, 5'-CAC GGA TCC TGA CGA CTG AC-3'; N70DNA,

5'-GGG AGA GCC ATA CCT GAC-N70-CAG GTT ACG CAT CC-3'; and N72DNA, 5'-CAC GGA TCC TGA CGA CTG AC-N72-GGA TGC GTA ACC TG-3' were synthesized, purified and used in a large scale PCR amplification reaction to generate a full-length 222-mer double-stranded DNA pool as described previously [21]. For *in vitro* transcription, 3.6 nmol of PCR-amplified DNA pool was used in a 3.5-ml transcription reaction (40 mM Tris-HCl pH 8.0, 12 mM MgCl₂, 2 mM spermidine, 50 mM NaCl, 30 mM dithiothreitol, 5 mM ATP, CTP, UTP, 2 mM GTP, 3 mM initiator nucleotide, 3 μM [α -³²P]GTP (0.2 μCi/μl), 5 U/μl T7 RNA polymerase) and transcribed at 37°C for 4 h. 300 U DNase I was added and incubation was continued for 30 min. RNA was purified on a 5% denaturing polyacrylamide gel, visualized, excised, eluted and precipitated and used for selections. The fraction of RNA derivatized with the fumaramide moiety at the 5'-end was found to be 40% by electrophoretic polyacrylamide gel retardation assays (data not shown).

5.3. Preparation of the biotin cysteine substrate

The biotin cysteine substrate was synthesized with a trityl-protection group at the sulfur to avoid disulfide-formation during storage and a Boc-protecting group at the α -amino group. Before the substrate could be used in the selection experiment, it was deprotected with trifluoroacetic acid. Therefore 10–70 mg of the double protected biotin cysteine were dissolved in 500 μl of methylene chloride and 2.5 mol equivalents of triethylsilane and 500 μl of trifluoroacetic acid were added. After 20 min, the reaction mixture was concentrated by speed vac evaporation to a dry pellet, which was redissolved in 500 μl distilled water and adjusted to pH 7.4 by titration with 10 M KOH.

5.4. *In vitro* selection

In vitro selection was performed with an initial pool of approximately 2×10^{15} sequences using an average of four copies of each molecule in the first cycle. The RNA library was heated to 94°C for 5 min in Mg²⁺-free selection buffer containing 200 mM NaCl, 50 mM K-MOPS, pH 7.4 to denature the RNA. The concentration of MgCl₂ was then adjusted to 5 mM and the reaction mixture was cooled down to room temperature for 20 min to allow proper folding of the RNA molecules. The reaction was then initiated by the addition of the substrate to give a final concentration of 2 mM and incubated at room temperature for 1 h. Selection stringency was gradually increased by decreasing the biotin cysteine concentration to 100 μM and the incubation time to 1 min (see Fig. 2). To remove the large excess of biotinylated cysteine the reaction mixture was filtered through a Sephadex G-50 column. Fractions containing RNA were then ethanol-precipitated, resuspended in 200 μl of streptavidin binding buffer (150 mM NaCl, 25 mM NaH₂PO₄, pH 6.9) and incubated with 200 μl of a 50% slurry of streptavidin agarose for 30 min. The sample was transferred to a spin filter and washed 20 times with four column volumes of denaturing buffer (8 M urea, 5 mM EDTA, adjusted with K-MOPS to pH 7.4) and twice with water.

RNAs linked to the streptavidin resin were directly reverse-transcribed according to the manufacturer's instructions. Reverse-transcribed RNA was PCR-amplified and T7-transcribed. Beginning with round 3, a second selection ('UV-cleavage' selection), also deriving from DNA pool of selection cycle 2, was performed in parallel by introducing an additional elution step into the protocol: after the washings the immobilized RNA molecules were eluted by photoirradiation with UV-light. For this purpose the washed streptavidin matrix was resuspended in 400 μl, cooled on ice and directly exposed to light at 366 nm of a 15 W UV-lamp for 3 h. Afterwards the agarose was transferred to a spin filter and subsequently washed for two times with four column volumes of water. The flow through and the two washing fractions were taken together, ethanol-precipitated, washed for two times with 70% of ethanol, resuspended in water and reverse-transcribed. Beginning with round 7, in every other round a pre-selection step against streptavidin agarose was introduced in both selections: after the initial denaturation step, RNA was cooled on ice and incubated with streptavidin agarose for 45 min. The supernatant was heated to 95°C for 5 min and cooled to room temperature for 20 min again, followed by the selection procedure as described above.

Apparent rate constants k_{app} were calculated from the percentage of immobilized RNA (IM) using Eq. 1:

$$k_{app} = 1/t([BC]_0 - [F - RNA]_0) \times \ln \left(\frac{[F - RNA]_0 [BC]_t}{[F - RNA]_t [BC]_0} \right) \quad (1)$$

in which [BC]₀ and [F-RNA]₀ are the initial concentrations of biotin cysteine and fumaramide-RNA, respectively, and the concentrations of fumaramide-RNA and biotin cysteine at the time t . [F-RNA] _{t} and [BC] _{t} were calculated from Eqs. 2 and 3:

$$[F - RNA]_t = ((100 - IM)/100) [F - RNA]_0 \quad (2)$$

$$[BC]_t = [BC]_0 - [F - RNA]_0 + [F - RNA]_t \quad (3)$$

Pool DNAs obtained after round 14 of the 'UV-cleavage' selection and DNA pool 16 of the 'direct amplification' selection were cloned and sequenced as described [30].

5.5. Kinetic assays

All kinetic experiments were carried out at a concentration of 1 μM of substrate-derivatized UV5 ribozyme in selection buffer at room temperature. T7 transcriptions for the production of RNAs, primed with derivatives 2, 3, 4 of the fumaramide moiety were carried out under the same conditions as described for the selection experiment. RNAs were radioactive 3'-end-labelled by standard protocols. Reactions were performed in 100 μl volumes at concentrations of biotin cysteine in the range of 50–1000 μM for Michaelis–Menten kinetics. 20 μl aliquots were taken at eight different time points and reactions were stopped by ethanol precipitation. Biotinylated RNAs were coupled to streptavidin agarose by incubating the samples with 60 μl of swollen resin for 30 min. Reaction mixtures containing more than 100 μM of biotinyl-

ated substrate were passed over a Sephadex G-50 column prior to streptavidin coupling. The resin was then transferred to a spin filter tube and washed extensively with denaturing buffer. The amount of biotinylated RNA was quantified by counting the radioactivity of flow through and streptavidin resin in a scintillation counter (Packard). Initial rates were calculated from these data by curve fitting (see Fig. 8). No more than 60% of enzyme reacted during the course of these assays. Intermolecular reactions were performed in 50 μ l volumes at [ribozyme 20–188]=0.2–4.0 μ M, at a concentration of 4 nM of radioactive 3'-end-labelled 20-mer (5'-GGG AGA CCA UAC CUG ACC CG-3'), and [biotinylated cysteine]=0.5, 1, 2, 5, and 10 mM. 5- μ l aliquots were taken at 10 different time points and reactions were stopped by mixing the aliquots with 5 μ l PAGE loading buffer each (9.0 M urea, 20 mM EDTA) and freezing to -80°C . Samples were analyzed on a denaturing 20% polyacrylamide gel and quantified on a phosphor imager (Fuji). Values of k_{obs} were determined from these data by curve fitting (see Fig. 8). Inhibition reactions were performed using 0.1, 1, 5, 10 and 25 mM biotin, respectively 10 mM acyl cysteine or cysteine, 1 μ M ribozyme UV5 and 0.1 mM biotin cysteine at 5 mM MgCl_2 . Aliquots were taken at five different time points and analyzed as described for the intramolecular reactions. Values of K_i were obtained from these data by non-linear least square curve fitting using the equation $k_{\text{obs}} = k_0/(1+[I]/K_i)$, where k_{obs} is the observed rate constant, k_0 is the rate of the uninhibited reaction, $[I]$ is the concentration of inhibitor, and K_i is the concentration that yields half-maximum inhibition.

5.6. Production of short RNase H cleavage products for MALDI-ToF analysis

For the production of short RNA oligomers comprising of the first 28, 29 and 30 nucleotides of the ribozyme UV5 RNA, 5 nmol of fumaramide-derivatized and biotinylated ribozyme RNA were digested with 40 units RNase H destroying the RNA strand of RNA•DNA hybrids marked by hybridization from nucleotide position 20–40, 20 nucleotides downstream of the 5'-end of the ribozyme UV5 RNA to the complementary DNA oligonucleotide UV5 20.21–40 (5'-CCA TCC CTG TCA GAC AAA CC-3'). 5 nmol of biotinylated RNA were produced in a 8 ml ribozyme reaction using 1 mM of biotinylated cysteine, 1 μ M ribozyme UV5 at 12 mM MgCl_2 . Molecules linked to the streptavidin resin were eluted with 2 M 2-mercaptoethanol [21], lyophilized, and resuspended in water. The RNase H reactions contained 16 μ g of RNA (250 pmol), 1 nmol of UV5 20.21–40 oligonucleotide, 50 mM Tris-HCl at pH 8.3, 75 mM KCl and 3 mM MgCl_2 . After preincubation at 72°C for 3 min to denature strands, the solution was incubated at 37°C for 30 min for hybridization and the enzyme was added. The reaction was held at 37°C for 3 h and then was stopped by addition of 10 mM EDTA. Non-biotinylated and non-primed short RNA cleavage products were separated and purified on a 12% polyacrylamide gel. Biotinylated short cleavage products were immobilized on streptavidin agarose, washed with denaturing buffer, eluted with 2-mercaptoethanol, desalted and lyophilized.

5.7. Structural characterization of UV5 ribozyme by enzymatic probing

The enzymatic characterization of the secondary structure of the ribozyme was performed by employing structure- or base-specific ribonucleases. RNase T1 hydrolyzes specifically single-stranded RNA (ssRNA) at guanosine positions. Nuclease S1 performs the same reaction without preference for certain bases. Nuclease S1 requires Zn^{2+} ions as a cofactor. For the partial digest approximately 10000 cps (5 pmol) of radioactive 5'- or 3'-end-labeled ribozyme was incubated with 5 U of the appropriate RNase in reaction buffer (4.3 mM Na_2HPO_4 pH 7.3, 3 mM MgCl_2 , 147 mM NaCl, 2.7 mM KCl, 1.4 mM KH_2PO_4 , 4 mM DTT) for 1 and 7 min, respectively. Samples for the RNase T1 digest contained 300 mM NaCl and samples of the RNase S1 reaction 1 mM ZnCl_2 . Both reactions were terminated by addition of 15 μ l stop solution (4 mg/ml proteinase K, 1% SDS, 1 mg/ml tRNA, 0.4 M NaOAc pH 5.3) and subsequent incubation for 1 h at 65°C . S1-Nuclease was inactivated by addition by 1 μ l 0.5 M EDTA (pH 8.0). After phenol/chloroform extraction nucleic acids were loaded on a denaturing 12% polyacrylamide gel.

Acknowledgements

We thank O. Thum, A. Marx, S. Jäger, G. Mayer, and N. Raffler for helpful suggestions, M. Rehers and L. Hötzer for excellent technical assistance. We are grateful to D. Messina (Eurogentec, Belgium) for performing MALDI-TOF analyses. This study was supported by a grant from the Deutsche Forschungsgemeinschaft to M.F.

References

- [1] M. Koizumi, G.A. Soukup, J.N.Q. Kerr, R.R. Breaker, Allosteric selection of ribozymes that respond to the second messengers cGMP and cAMP, *Nat. Struct. Biol.* 6 (1999) 1062–1071.
- [2] N. Piganeau, A. Jenne, V. Thuillier, M. Famulok, An allosteric ribozyme regulated by doxycycline, *Angew. Chem. Int. Edn.* 39 (2000) 4369–4373.
- [3] T. Tanabe, T. Kuwabara, M. Warashina, K. Tani, K. Taira, S. Asano, Oncogene inactivation in a mouse model, *Nature* 406 (2000) 473–474.
- [4] D.P. Bartel, P.J. Unrau, Constructing an RNA world, *Trends Cell Biol.* 9 (1999) M9–M13.
- [5] G.F. Joyce, Building the RNA world, *Ribozymes Curr. Biol.* 6 (1996) 965–967.
- [6] R.F. Gesteland, T.R. Cech, J.F. Atkins (Eds.), *The RNA world*, 2nd edn., Cold Spring Harbor Laboratory Press, Cold Spring Harbor, NY, 1999.
- [7] T. Pan, Novel and variant ribozymes obtained through in vitro selection, *Curr. Opin. Chem. Biol.* 1 (1997) 17–25.
- [8] R.R. Breaker, In vitro selection of catalytic polynucleotides, *Chem. Rev.* 97 (1997) 371–390.
- [9] G.J. Narlikar, D. Herschlag, Mechanistic aspects of enzymatic catalysis: Lessons from comparison of RNA and protein enzymes, *Annu. Rev. Biochem.* 66 (1997) 19–59.
- [10] M. Famulok, A. Jenne, Catalysis based on nucleic acid structures, *Top. Curr. Chem.* 202 (1999) 101–131.

- [11] M.P. Sibi, S. Manyem, Enantioselective conjugate additions, *Tetrahedron* 56 (2000) 8033–8061.
- [12] S. Shimizu, S. Shiozaki, T. Ohshiro, H. Yamada, Occurrence of *S*-adenosylhomocysteine hydrolase in prokaryote cells. Characterization of the enzyme from *Alcaligenes faecalis* and role of the enzyme in the activated methyl cycle, *Eur. J. Biochem.* 141 (1984) 385–392.
- [13] J.R. Requena, M.X. Fu, M.U. Ahmed, A.J. Jenkins, T.J. Lyons, J.W. Baynes, S.R. Thorpe, Quantification of malondialdehyde and 4-hydroxynonenal adducts to lysine residues in native and oxidized human low-density lipoprotein, *Biochem. J.* 322 (1997) 317–325.
- [14] M. Sugumaran, V. Semensi, H. Dali, K. Nellaippan, Oxidation of 3,4-dihydroxybenzyl alcohol: a sclerotizing precursor for cockroach ootheca, *Arch. Insect Biochem. Physiol.* 16 (1991) 31–44.
- [15] C.W. Carreras, D.V. Santi, The catalytic mechanism and structure of thymidylate synthase, *Annu. Rev. Biochem.* 64 (1995) 721–762.
- [16] W.R. Montfort, K.M. Perry, E.B. Fauman, J.S. Finer-Moore, G.F. Maley, L. Hardy, F. Maley, R.M. Stroud, Structure, multiple site binding, and segmental accommodation in thymidylate synthase on binding dUMP and an anti-folate, *Biochemistry* 29 (1990) 6964–6977.
- [17] C.T. Walsh, *Enzymatic Reaction Mechanisms*, W.H. Freeman and Company, San Francisco, CA, 1979.
- [18] A.W. Schwartz, G.J. Chittenden, Synthesis of uracil and thymine under simulated prebiotic conditions, *Biosystems* 9 (1977) 87–92.
- [19] A.S. Choughuley, A.S. Subbaraman, Z.A. Kazi, M.S. Chadha, A possible prebiotic synthesis of thymine: uracil-formaldehyde-formic acid reaction, *Biosystems* 9 (1977) 73–80.
- [20] F. Hausch, A. Jäschke, Libraries of multifunctional RNA conjugates for the selection of new RNA catalysts, *Bioconjug. Chem.* 8 (1997) 885–890.
- [21] B. Zhang, T.R. Cech, Peptide bond formation by in vitro selected ribozymes, *Nature* 390 (1997) 96–100.
- [22] A.E. Walter, D.H. Turner, J. Kim, M.H. Lyttle, P. Muller, D.H. Mathews, M. Zuker, Coaxial stacking of helices enhances binding of oligoribonucleotides and improves predictions of RNA folding, *Proc. Natl. Acad. Sci. USA* 91 (1994) 9218–9222.
- [23] A. Jenne, M. Famulok, Disruption of the streptavidin interaction with biotinylated nucleic acid probes by 2-mercaptoethanol, *Biotechniques* 26 (1999) 249–254.
- [24] C. Wilson, J. Nix, J. Szostak, Functional requirements for specific ligand recognition by a biotin-binding RNA pseudoknot, *Biochemistry* 37 (1998) 14410–14419.
- [25] T.M. Tarasow, S.L. Tarasow, B.E. Eaton, RNA-catalysed carbon-carbon bond formation, *Nature* 389 (1997) 54–57.
- [26] T.W. Wiegand, R.C. Janssen, B.E. Eaton, Selection of RNA amide synthases, *Chem. Biol.* 4 (1997) 675–683.
- [27] B. Seelig, A. Jäschke, A small catalytic RNA motif with Diels-Alderase activity, *Chem. Biol.* 6 (1999) 167–176.
- [28] C. Wilson, J.W. Szostak, In vitro evolution of a self-alkylating ribozyme, *Nature* 374 (1995) 777–782.
- [29] S.A. Benner, A.D. Ellington, A. Tauer, Modern metabolism as a palimpsest of the RNA world, *Proc. Natl. Acad. Sci. USA* 86 (1989) 7054–7058.
- [30] M. Famulok, Molecular recognition of amino acids by RNA-aptamers – an L-citrulline binding RNA motif and its evolution into an L-arginine binder, *J. Am. Chem. Soc.* 116 (1994) 1698–1706.